

Seismic, geologic, geomechanics, and dynamic constraints in flow models of fractured reservoirs

Reinaldo J. Michelena* and James R. Gilman, *iReservoir.com, Inc.*

Chris K. Zahm, *Bureau of Economic Geology, University of Texas at Austin*

Summary

In this paper we present a workflow to build permeability models for flow simulation in naturally fractured reservoirs constrained by 3D seismic, geologic data and concepts, geomechanics observations, and dynamic data. Joints and faults are modeled separately to account for their differences in scale and flow properties. Seismic-derived orientation statistics are compared against orientations from outcrops and microseismic data to assess their validity and consistency across multiple scales. We show the impact of natural fractures and stress orientation in the flow and variability of the pressure field around producing wells in an unconventional reservoir. Such variability can have a significant impact on well interference and optimal well spacing.

Introduction

Understanding of natural fractures in conventional and unconventional reservoirs is important because natural fractures may enhance fluid flow from the matrix into the wellbore and play an important role in hydraulic fracture stimulation.

Fluid flow in natural fractures depends on how the fractures were originated (e.g. extension versus shear), their geometry, spatial distribution, and their quality. Fracture quality (i.e., flow capacity potential) is determined by current stress conditions and diagenetic alterations that may have occurred to the fractures after their formation (National Research Council, 1996).

Fluid flow in naturally fractured reservoirs is not only controlled by fracture properties but also by matrix properties, fluid pressure-volume (PVT) behavior, stimulation parameters, and their interaction. In order to understand these complex interactions, we use flow simulation, first, to calibrate all the concepts incorporated into geological and dynamic models and, second, to understand the nature of the production decline.

In this paper, we present a workflow to extract, map, and calibrate natural fractures from 3D seismic data that are used to constrain fracture modeling and flow simulation models. Extensional fractures (joints) and shear fractures (faults) are modeled separately to account for their different sizes and flow properties in the flow simulator and to assess their relative importance when calibrating with production data. Once the seismic derived fracture information has been properly calibrated, we briefly explain how to upscale

fracture models for effective permeability introducing the effect of current day earth stress. We then illustrate the dynamically-modeled heterogeneity in the pressure field that results after incorporating all the complexities in matrix and natural fracture variability.

Fracture modeling workflow

Our fracture modeling workflow emphasizes the parameters that control fluid flow (geological origin of the fractures, distribution and geometry, and fracture quality) and leave open the possibility of testing the relative importance of each of these parameters by calibrating with actual production data in the flow simulator.

We first generate separate models for fractures of different sizes. Joints (or bed-bound fractures) and small faults (sometimes referred to as through-going fractures) are defined separately to be able to account for their significant differences in flow properties (Figure 1). Although joints (controlled by rock properties, mechanical stratigraphy, bed thickness and stress state) may have diminished apertures at depth, they may still enhance fluid flow in rocks with almost no matrix permeability (Zoback, 2007) and their importance should be evaluated. Through-going fractures (controlled by seismic/sub-seismic scale faults and stress) tend to show significantly higher permeability than joints and may enhance vertical communication between reservoir compartments with different rock properties (Figure 1).

We constrain the geometry of the fractures by using intensity, orientation, and Fisher coefficient extracted from structural seismic attributes (Michelena et al., 2013). We also extract information about families of orientations whose flow properties can vary in the flow simulator to better calibrate with production data. If discrete fracture models are generated, parameters such as height, fracture length, and fracture aperture are also needed. These parameters can be extracted from bed thickness from logs and outcrop analogs.

Finally, after we model different fracture types by origin with their corresponding geometry and spatial distribution, we estimate their quality based on their relative orientation to current earth stress state and assessment of any diagenetic process that may have altered the initial void space between fracture surfaces. Often, fractures that are hydraulically conductive are those that are critically stressed in the current stress field (Zoback, 2007). Therefore, besides the origin of the fractures, knowledge of

Constrained flow models in naturally fractured reservoirs

the current stress field can help separate fractures between more and less conductive depending (mostly) on their relative orientation with respect to the maximum horizontal stress. Dynamic well tests are used in this step to calibrate effective permeabilities.

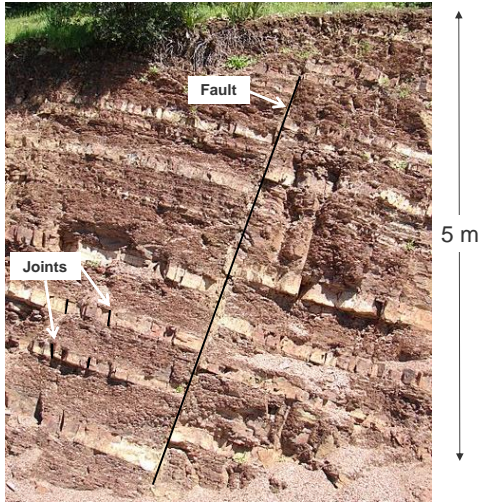


Figure 1: Outcrop showing joints and faults in a sandstone/mudstone sequence. Notice the differences between the two regarding their number, relation to rock properties of individual layers, and vertical connectivity. Both types of fractures are below seismic resolution but have very different flow properties. Modified from Bouttemy (2013).

Natural fracture attributes from seismic

An important component in our workflow is the estimation of the heterogeneity on the distribution of natural fractures based on seismic data. The actual steps followed to model natural fractures constrained by seismic data depends on the origin of the fractures, the available seismic data, and the independent fracture data that we use for calibration.

Since mechanical rock properties control the distribution of joints, we first perform mechanical facies modeling constrained by facies probabilities derived from prestack inversion results (Michelena et al., 2017). By using mechanical facies that are more or less prone to fractures, we take into account the bed-bound nature of the joints whose growth is controlled by mechanical properties. Different facies are assigned different fracture intensities. These intensities are weighted by distance to fault functions that vary by facies to account for the observed mechanically-dependent fracture intensity decay away from faults (Caine et al., 1996). Strain derived from seismic dip attribute may also be used to weight the relative intensities of joints across the area of interest by assigning higher intensities to areas of higher dip. The result is a model for

joints that (statistically) honors the well data in terms of intensity and layer thickness and shows the expected behavior with respect to distance to faults and strain.

Small faults are mostly independent of rock properties and are modelled by using structural seismic attributes (which tend to highlight large-scale structural features). The selection of the attribute should be performed after careful calibration with independent fracture data. The selected attribute will determine the final distribution of the modeled faults. Three attribute volumes are extracted from the structural attribute of choice: dominant local strike, Fisher coefficient, and intensity (Michelena et al., 2013). Orientations can be used to generate separate models for different fracture families that, if needed, may also have different flow properties in the simulator.

Regarding the orientation of the joints, and if not azimuthal prestack data is available, we assume that the orientations of joints and through-going fractures share the same statistics (a hypothesis that must be validated locally). If azimuthal prestack data is available, we can use the orientations derived from AVAZ analysis to constrain the orientations of joints (after proper QC with independent fracture data). We must be aware, however, that the model driven nature of AVAZ analysis may yield erroneous results if the actual fracture geometry differs from the assumed fracture model. We must also keep in mind that azimuthally anisotropic parameters derived from prestack seismic data are influenced by both joints and small faults, may be sensitive to stress anisotropy, and may vary with rock properties. The relative importance of these effects in the observed seismic anisotropy must be quantified.

Field data example

This section shows an example of the application of the workflow described above in an unconventional reservoir located in South Texas. 3D seismic data that covers an area of 280 square miles was available for this study. A detailed reservoir characterization and flow simulation study was performed in a smaller 3.6 square miles area highlighted in Figure 2. Maximum curvature was extracted from the 3D seismic data and used to extract local strike orientations (Figure 2). Orientations were statistically analyzed in 11x11 superbins and the count of the different angles was used to estimate local fracture intensities and to separate different families (similar to how fracture intensities and families are estimated by counting angles from FMI data). As Figure 2 shows, two main families of orientations (green and yellow) can be identified from the seismic data.

Before the statistics of strikes can be used to constrain the model of natural fractures, we must check whether these orientations are related to expected orientations of actual

Constrained flow models in naturally fractured reservoirs

natural fractures. A detailed outcrop description of the reservoir interval was available from a separate study (Ferrill, 2014) and we used its findings to QC the seismic-derived orientations. As Figure 3 illustrates, two families of joints are observed. Their orientations and relative intensities coincide with the families of fault orientations derived from seismic data (Figure 2).

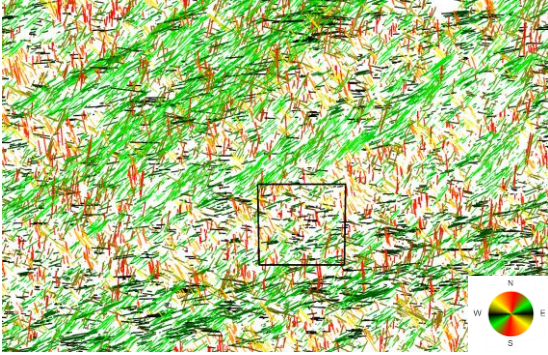


Figure 2: Detail of local strike orientations in an area of 280 sqm. The area of interest for the simulation study (in black) is about 3.6 sqm. The dominant orientation is around N45E (green) with a secondary orientation around N45W degrees (yellow). Portions of the seismic data owned or controlled by Seismic Exchange, Inc. and Seitel; interpretation is that of iReservoir.

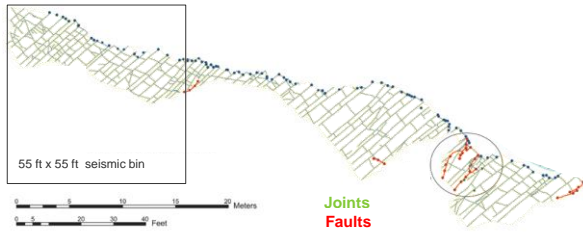


Figure 3: Map view of interpreted joints and faults from outcrop (modified from Ferrill et al., 2014). The orientation of the dominant joint set is about N45E and the secondary set is about N45W. Faults (in red) also show similar orientations. Compare with seismic derived orientations in Figure 2. AAPG ©2014, reprinted by permission of the AAPG whose permission is required for further use.

Microseismic data along five horizontal wells recorded with a surface array were also available in this area. A histogram of the orientations of microseismic events is shown in Figure 4. Notice that microseismic derived orientations also show the same two families of fractures observed in the outcrop, the large seismic area, and the area of interest, which confirms that seismic derived orientations and relative intensities derived from seismic are adequate to constrain the fracture models for both joints and faults.

Intensities of joints were guided by a model of mechanical facies constrained by prestack inversion results. Joint

height and spacing were also controlled by bed thickness and fault proximity. Intensities of faults were further scaled by fault proximity. Figure 5 shows the discrete fracture models for joints and faults that resulted from this workflow.

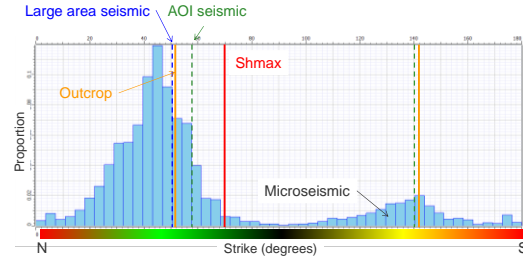


Figure 4: Histogram of fracture orientations from microseismic data. Dominant orientations extracted from outcrop, large 3D seismic area and smaller AOI are also posted for comparison. The same families of orientations are observed at all scales.

Model upscaling and effective permeability

Matrix and fracture porosity and permeability, fluid properties, and the interaction of all of the above are the parameters that control fluid flow in naturally fractured reservoirs. We built a model for *matrix* porosity and permeability using a workflow described in Michelena et al. (2017). This model was later upscaled for flow simulation. The natural fracture models shown in Figure 5 were also upscaled separately using the Oda equation (Oda, 1985). From the Oda equation we conclude that the effective fracture permeability tensor in a cell is proportional to the sum of the product of individual fracture permeabilities, fracture porosity, and a geometric factor related to the (seismic derived) fracture orientations, as follows:

$$k_{eij} \propto \sum_{k=1}^{N_f} \left(\frac{w_f^2}{12} \right)_k \left(\frac{w_f A_f}{\Delta x \Delta y \Delta z} \right)_k (n_i n_j)_k, \quad (1)$$

where k_{eij} is the effective perm in a cell that is crossed by N_f fractures, w_f is the fracture width, A_f is the fracture area, $\Delta x \Delta y \Delta z$ is the cell volume, and n_i is the projection of the normal to the fracture k along the i_{th} axis. Notice that the effective perm is proportional to the cube of the fracture width w_f of the individual fractures (a relation also known as “cubic law”). This type of relation results in w_f playing a dominant role in determining which fracture has a larger contribution to the overall effective perm when a cell is crossed by several natural fractures. Fracture width, in turn, depends on current stress state and diagenetic alterations that may have filled the initial void space. By assuming that fracture porosity is small (typically a fraction of 1%), equation 1 can be calibrated with dynamic well test data to estimate a “hydraulic aperture” for conductive fractures.

Constrained flow models in naturally fractured reservoirs

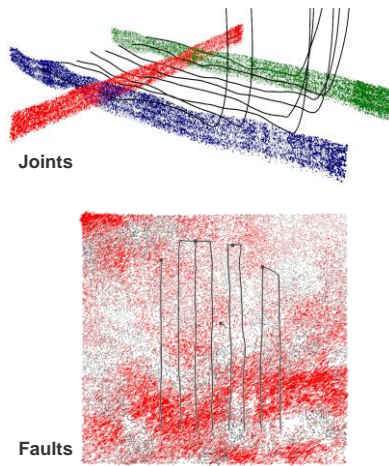


Figure 5: Discrete fracture models for joints and faults. Two families of orientations are modeled for each type of fracture. Rock properties control the vertical intensity of joints. Distance to large faults also affects the intensity of joints and faults.

To better understand the relationship between effective permeability and stress (equation 1), we modeled the effect of stress by changing the fracture width with respect to the angle between S_{Hmax} and each fracture strike for different fracture geometries. Figure 6 (left) shows the orientation of the maximum perm K_{max} (determined from the effective permeability tensor) when equal fracture widths are used for all fracture orientations to simulate an isotropic stress field. In this case, the orientation of K_{max} coincides with the orientations of the most intense fractures. Figure 6 (right) shows the result of assuming an anisotropic aperture function. In this case, the orientation of K_{max} is closer to the fractures with wider apertures (critically stressed) even if they are less intense. Due to the cubic law, the wide, critically stressed fractures in this example are 27 (3^3) times more conductive than the thin ones, which explains the disproportional contribution of the less intense fractures into the effective flow. For this reason, and since the widths of joints are expected to be smaller than the widths of critically stressed faults, the contribution of joints to the effective fracture perm was also considered small; we added their contribution to the matrix perm to create an “enhanced” matrix. Only small faults were included in the final fracture model for calibration with dynamic data.

An example of the pressure field from dual-permeability flow simulation after history matching rate, pressure decline, and observation well pressures is illustrated in Figure 7. The use of matrix and fracture models generated in this study results in a heterogeneous pressure field, which contrasts with the idealized, elliptical SRVs often assumed to describe drainage patterns in unconventional reservoirs. Such variability can have a significant impact on well interference and optimal well spacing.

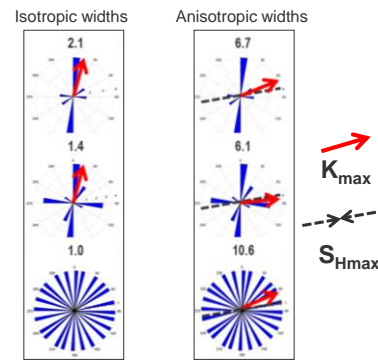


Figure 6: Rose diagrams of different scenarios of families of open vertical fractures. Left: orientation of maximum horizontal perm K_{max} (red) assuming an isotropic aperture distribution. Right: orientation of K_{max} assuming an anisotropic aperture distribution (0.3 mm for critically stressed fractures and 0.1 mm for non-conductive fractures). Numbers above each rose diagram indicate the corresponding perm anisotropy K_{max}/K_{min} .

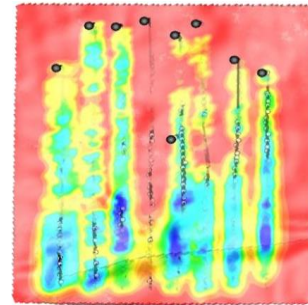


Figure 7: Plan view of the average pressure field around horizontal wells in the reservoir estimated from dual-permeability flow simulation after history matching. Red color represents initial pressures.

Conclusions

We have presented a seismic constrained geological modeling workflow in naturally fractured reservoirs that takes into account the geologic, geomechanics, and dynamic parameters that control fluid flow. Calibration with independent information is important to increase confidence in the results. The pressure field that results after performing flow simulation using this seismically constrained model is significantly heterogeneous, impacting long-term well interference.

Acknowledgments

We thank BHP Petroleum for permission to publish these results and Mauricio Florez for his support during this project. Thanks to Li-Wei Cheng for his help in estimating K_{max} using the Oda equation.

REFERENCES

- Bouttemy, F., 2013, Faille dans les terrains Carbonifère, <https://www.geodiversite.net/media1015>.
- Caine, J. S., J. P. Evans, and C. B. Forster, 1996, Fault zone architecture and permeability structure: *Geology*, **24**, 1025–1028, [https://doi.org/10.1130/0091-7613\(1996\)024<1025:fzaaps>2.3.co;2](https://doi.org/10.1130/0091-7613(1996)024<1025:fzaaps>2.3.co;2).
- Ferrill, D. A., R. N. McGinnis, A. P. Morris, K. J. Smart, Z. T. Sickmann, M. Bentz, D. Lehrmann, and M. A. Evans, 2014, Control of mechanical stratigraphy on bed-restricted jointing and normal faulting: Eagle Ford Formation, south-central Texas, U.S.A.: *AAPG Bulletin*, **98**, 2477–2506, <https://doi.org/10.1306/08191414053>.
- Michelena, R. J., K. S. Godbey, and O. G. Angola, 2017, Integrated facies modeling in unconventional reservoirs using a frequentist approach: Example from a South Texas field: *Geophysics*, **82**, no. 6, B219–B230, <https://doi.org/10.1190/geo2017-0041.1>.
- Michelena, R. J., K. S. Godbey, H. Wang, J. R. Gilman, and C. K. Zahm, 2013, Estimation of dispersion in orientations of natural fractures from seismic data: Application to DFN modeling and flow simulation: *The Leading Edge*, **32**, 1502–1512, <https://doi.org/10.1190/tle32121502.1>.
- National Research Council, 1996, Rock fractures and fluid flow: contemporary understanding and applications: The National Academies Press.
- Oda, M., 1985, Permeability tensor for discontinuous rock masses: *Geotechnique*, **35**, 483–495, <https://doi.org/10.1680/geot.1985.35.4.483>.
- Zoback, M. D., 2007, Reservoir geomechanics: Cambridge University Press.